



Improving the Seismic Performance of Precast Post-Tensioned RC Shear Walls by Applying FRP Sheets

Sayed Mahdi Ghessisin¹, Babak Behforouz^{2*}, Farshid Fathi³, Saied Jalil Hosseini⁴

¹ Department of Civil Engineering, Najafabad Branch, Islamic Azad University, Najafabad, Iran

² Water Studies Research Center, Isfahan (Khorasgan) Branch, Islamic Azad University, Isfahan, Iran.

³ Department of Civil Engineering, Najafabad Branch, Islamic Azad University, Najafabad, Iran.

⁴ Department of Civil Engineering, Najafabad Branch, Islamic Azad University, Najafabad, Iran

Article Info

Received 20 December 2024
Accepted 20 February 2025
Available online 06 March 2025

Keywords:

Prestressing;
Post-tensioned;
Precast Concrete Shear Walls;
FRP Sheets;
Abaqus Software.

Abstract:

This paper refers to a finite element method-based parametric study of the influence of FRP sheets on the performance of post-tensioned RC shear walls due to lateral loads. Based on this, changes in length (85 and 170 cm), width (20 and 40 cm), and angle of FRP sheet arrangement relative to the horizontal axis (0°, 45° and 90°) have been used as parameters affecting the performance of post-tensioned RC shear walls against lateral loads. In this regard, an experimental campaign taken from the literature is introduced. A FE model is created to simulate the experiments. The results of these experiments are compared with the FE model for validation purposes. Afterwards, FRP sheets are incorporated into the FE model. The main innovation refers to a sensitivity analysis of the influence of different geometries of the FRP sheets on the performance of the wall. Results are obtained using FRP sheets for different parameters. It is concluded that FRP sheets exhibiting larger widths and inclinations correspond to a better lateral load-bearing capacity of the post-tensioned shear walls. This ductility increase varies from 1.5% to above and will reach nearly 10% at a 90-degree angle to the horizontal surface and with the largest width of the FRP sheet).

© 2025 University of Mazandaran

*Corresponding Author: babakbehforouz@gmail.com

Supplementary information: Supplementary information for this article is available at <https://cste.journals.umz.ac.ir/>

Please cite this paper as: Ghessisin, S. M. , Behforouz, B. , Fathi, F. , & Hosseini, S. J. (2025). Improving the Seismic Performance of Precast Post-Tensioned RC Shear Walls by Applying FRP Sheets. *Contributions of Science and Technology for Engineering*, 1(4), 35-43. doi:10.22080/cste.2025.28235.1006.

1. Introduction

Post-tensioned precast reinforced concrete shear walls are the primary elements resisting lateral loads in precast concrete structures [1, 2]. They resist lateral loads caused by earthquakes, and the floors sustain gravity loads [3, 4]. The lateral load-bearing capacity of the post-tensioned precast reinforced concrete shear walls can be determined by evaluating the laboratory results. It can be obtained by testing the laboratory samples subject to the increasing lateral horizontal force. In this type of wall, cracks generally disappear on the wall's surface. They are due to tensile stresses caused by shear and bending forces [5]. Consequently, reaching the tensile stresses to the yield stress causes concrete crushing [6, 7]. This is one of the main reasons for the decrease in the capacity of post-tensioned precast reinforced concrete shear walls. These cracks begin from the boundary elements, perpendicular to them, and extend from a distance of about (where d is the depth of the boundary elements) at approximately the vertical extension toward the lower part of the wall. According to the concrete's crack distribution and failure mechanism, the

wall can be strengthened by attaching FRP sheets with a special arrangement. The FRP sheets delay cracking caused by bending and shear stresses and improve their lateral-load-bearing performance. For these reasons, this method has been widely utilized in recent years to improve the lateral-load bearing performance of shear walls [8-12]. Studying this subject originated in the mid-nineties [13-16]. Mander and Cheng proposed the damage avoidance design based on the termination of the longitudinal column reinforcement at the foundation beam-column interface. This termination allows the column to rock freely. In this case, the post-tensioned precast reinforced concrete shear wall is subject to earthquake-cyclic forces and swings like a cradle on the foundation beam. The earthquake energy would be dissipated because of plastic deformation created in the embedded steel bars located in the connection point of the wall and the foundation beam [17]. Priestley et al. designed, built, and tested a five-story precast building subject to simulated seismic loading [18]. The test results revealed minimal damage in the wall direction, with a roof drift ratio of 1.8%. Some minor flexural cracking and minor



cover concrete crushing are evident at the base of the wall. Another study was conducted to guide the design of precast hybrid frames and joint wall systems [19]. The research carried out further led to the publication of new and practical design guidelines, including ACI ITG 5.1 & ACI ITG 5.2, in post-tensioned precast reinforced concrete shear walls [20-22]. Kurama et al. assessed the behavior of post-tensioned precast concrete walls subject to lateral load and proposed a seismic design approach. The study proposes four states of precast wall lateral force-displacement response [21]. Holden et al. evaluated two geometrically identical half-scale precast concrete cantilever wall units subject to quasi-static reversed cyclic lateral loading [22]. One of them was a sample of a conventional reinforced concrete shear wall constructed at a construction site. It was in accordance with the existing design guidelines. Another case was constructing a precast reinforced concrete shear wall sample containing prestressed carbon tendons and steel fibers. After the tests, the results showed that despite the appropriate lateral-load bearing performance, the first type of wall collapsed after reaching a drift of 2.5%. However, the second wall has not undergone significant structural changes after reaching 3% drift. In another study, Restrepo and Rahman investigated three half-scale precast concrete wall units with identical reinforcement details, including similar prestressing strand arrangements and fully equal loading patterns, in a 4-story building through quasi-static reverse cyclic loading. All of them were designed with conventional rectangular transverse reinforcement and longitudinal bars; the test was continued until the specimens reached a drift of 2.5%. They observed only very minor changes in appearance at the toes of the walls, and the prestressing strands remained in the elastic region with no residual drift. The energy dissipation bars worked very well, resulting in a viscous damping ratio of 14% [23]. Continuing the research, Perez et al. presented an analytical model based on a simple and common design process, using applied formulas, to investigate the lateral-load bearing performance of post-tensioned precast concrete walls under lateral loads and design criteria. The results of the analysis showed a very good agreement with the existing experimental findings. Analytical and experimental results showed a good agreement between the three samples that were subjected to uniform and cyclic loading. The proposed model was very efficient for the seismic design of post-tensioned precast concrete walls [24]. Next, in 2013, this researcher and his colleagues tested five prestressed concrete walls made with real scale in a laboratory study. These walls were tested with appropriate supports on multiple floors, without connecting beams, with horizontal joints under combined gravity and lateral loading. The results show that based on the predictions made in the design, the limit state of the functional range of the wall is determined in terms of seismic responses. In addition, the results of this research showed that these walls can undergo significant nonlinear lateral drifts while maintaining their self-centering characteristics. This performance is while the walls were not significantly damaged [25]. Tanyeri assessed the effect of four design parameters in post-tensioned precast reinforced concrete shear walls, including the post-tensioned steel total surface, the post-tensioned steel initial

stress, the initial concrete stress due to the post-tensioning, and the stirrups detail in the boundary elements, subject to lateral displacement [18]. The results indicate that reducing the initial tension of the concrete reduces the displacement caused by the opening of the gap and the base shear on the surface of the concrete cover. This reduction is due to reducing the post-tensioned tendons' initial prestress [19]. Zhu and Guo run experiments on Hybrid Precast Walls by Emulating Monolithic (HPWEM) construction [2]. They proposed an HPWEM construction, where the grouted vertical connecting reinforcements and high-strength post-tensioned steel strands are installed across the horizontal joint of the wall foot with the foundation beam. The overlapping welded closed stirrups improved the confinement property of the restrained concrete by avoiding brittle failure.

It can be said that FRP-strengthening of the walls prevents the expansion of cracks so that part of the tensile stresses caused by shear and bending forces in the wall plane is controlled by FRP sheets [26, 27]. This prevention increases the shear and bending capacity of the precast un-bonded post-tensioned reinforced concrete shear walls. Furthermore, recent research has investigated the seismic performance of composite coupled shear walls with varying CFRP sheet strengthening configurations under cyclic loading. This comparative study examined the ultimate capacity of RC shear walls coupled with CFRP sheets, comparing those initially loaded to 60% of their flexural capacity before strengthening with those strengthened from the outset. The results demonstrated a significantly higher seismic capacity in the strengthened structures compared to the unreinforced RC shear walls [28]. Another study in the same year investigated the efficacy of the EBROG method for enhancing the seismic performance of shear walls. Experimental results demonstrate that employing CFRP composites affixed to the concrete substrate via the EBROG technique substantially increases the strength, stiffness, ductility, and energy dissipation capacity of the reinforced concrete shear walls when subjected to seismic loading [29].

This study presents analytical models strengthened with FRP to assess and compare their efficiency in improving the behavior of precast concrete shear walls. To check the accuracy of the modeling, first, a computer model of the wall without FRP sheets is simulated and analyzed subject to the increasing lateral force. Next, the accuracy of the modeling is evaluated by comparing the analysis results with the laboratory results that were applied by Zhu and Guo [2]. After reviewing past research, in this research, a parametric study based on finite element modeling has been conducted. The results have been analyzed based on changes in length in the range of 85 to 170 cm, width of 20 to 40 cm, and the angle of the FRP sheet in relation to the horizontal axis from 0 to 90 degrees as available variables. In this regard, the performance of post-tensioned RC shear walls against lateral loads has been validated based on a laboratory model. Finally, the results of the models used were compared with each other. It should be noted that the main innovation of the research refers to the sensitivity analysis of the effect of different geometries of FRP sheets on the performance of the post-tensioned RC shear walls.

2. Modeling and Methods

2.1. Description of the Numerical Model

The distribution of cracks and the mechanism of concrete failure subject to the forces is illustrated in Figure 1. In this study, the three main analytical models that are strengthened with FRP are illustrated in Figure 2. In each model, the specifications of FRP sheets are considered variables such as width, length, and installation angle for the wall base. In these analyses, the loading is selected based on incremental horizontal displacements. In the first model in Figure (2-a), FRP sheets are attached from the two lower corners of the wall towards the center line on both sides of the shear wall with equal horizontal angles; in Figure (2-b), the FRP Sheets are glued in strips across the width of the shear wall parallel to the base of the shear wall and perpendicular to the boundary elements of the wall. In the third model, Figure (2-c), the FRP Sheets are added in strips perpendicular to the heel/toe of the shear wall along the boundary elements of the wall. The lateral-load bearing performance of the post-tensioned precast reinforced concrete shear wall is assessed. Due to the possibility of combining the first and second models, four main analytical models are assessed in ABAQUS software. In all cases, it is assumed that the main direction of FRP fibers is in the longitudinal direction of sheets. These fibers contribute to bearing the major share of tensile forces.

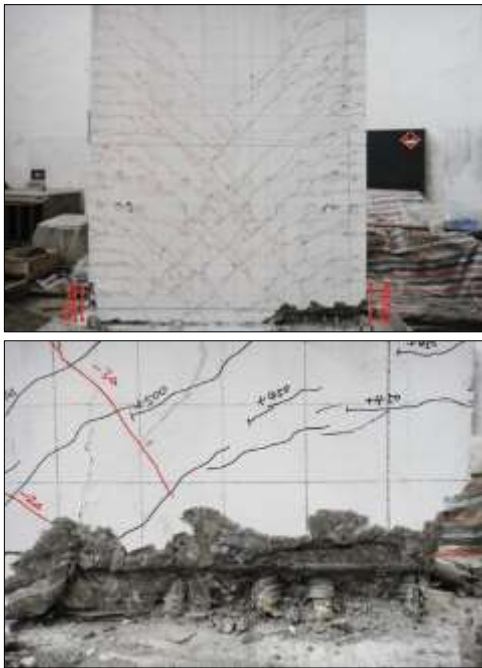


Figure 1. Wall crack pattern applied by Zhu and Guo [2]

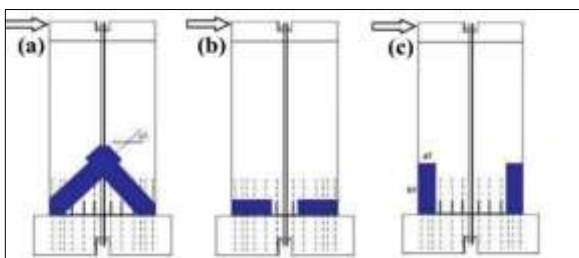


Figure 2. Arrangement of FRP plates to improve the post-tensioned precast reinforced concrete shear wall behaviour

To confirm the reliability of the results obtained from the FE models, they are validated through tests run on large-scale single post-tensioned precast RC shear walls [2]. These tests were done as part of an experimental and numerical study on the lateral-load-bearing performance of perforated, post-tensioned precast RC shear walls. The schematic view of the test sample, the HPWM6, and its dimensions are shown in Figure 3. The specifications of the materials consumed in the wall construction are illustrated below [2]:

1. Plain concrete with a grade of C35.
2. The average tensile properties of steel strands and reinforcements are tabulated in Table 1. The post-tensioned strand and stirrup bar did not have a considerable yield plateau, and their yield strength was taken as the proportional limit with a stress plastic strain of 0.2%.
3. A capping beam of 320mm height, 240mm width, and 1700mm length is fabricated on the top of the wall for hydraulic jack installation.
4. The concrete cover thickness is 15mm. Eight reinforcement rebar's of 16mm diameter are placed within the boundary elements at both wall toes. Eight reinforcement rebar's of 10mm diameter are embedded in the middle of the wall. The distributed horizontal reinforcements are arranged through the entire wall height in 200mm intervals with overlapping welded joints near the center of the wall. Stirrups of diameter 8mm with 135 hooks are located in the boundary elements at the wall toes in 100mm intervals.
5. The vertical reinforcements crossing the horizontal joint are anchored in grouted metal bellows embedded adjacent to the vertical reinforcements in the wall that provide a lap splice connection for the continuity of the reinforcements. The vertical reinforcements protruded 600mm from the top of the foundation beam. A portion of 150 mm length of these reinforcements is wrapped in plastic film.
6. Four high-strength strands of 15.2mm diameter are placed in an embedded PVC duct of 75mm diameter and passed through the wall panel, external beam, and foundation beam.
7. The space of exterior welded ties is reduced to 50mm [2].

The FRP material density is 1580 kg/m³. Table 2 provides the modulus of elasticity, Poisson's coefficient, and shear modulus of FRP sheets in different directions. As shown in Table 3, the tensile, compressive, and shear strength of FRP sheets in different directions are available [30]. According to the wall failure mode and the connection arrangement of the FRP sheets to the wall, these sheets should only be controlled in tensile mode. The wall failure mode of FRP is of tearing type, without separation and delamination, because the FRP material is not isotropic.

The primary variables of the FRP sheets are 1700 mm and 850 mm in length, 400 mm and 200 mm in width, with 1.4 mm thickness for all cases. It is assumed that the main

direction of the FRP sheets fibers is longitudinal, while the sticking angle to the wall base is at 0°, 45°, and 90°. A total of 13 samples are simulated for modeling and checking the sheet installation on the wall's surface relative to the horizon by computer (Table 3). Labeling the models begins with dfrp letters followed by six digits where the first two specify

the installation angle, the next two stand for the sheet width, and the last two are related to the length value. In this labeling, symbol X indicates the main direction of the fibers in the FRP sheet along its length, and the last digit is the thickness (i.e., dfrp02085x1.4)

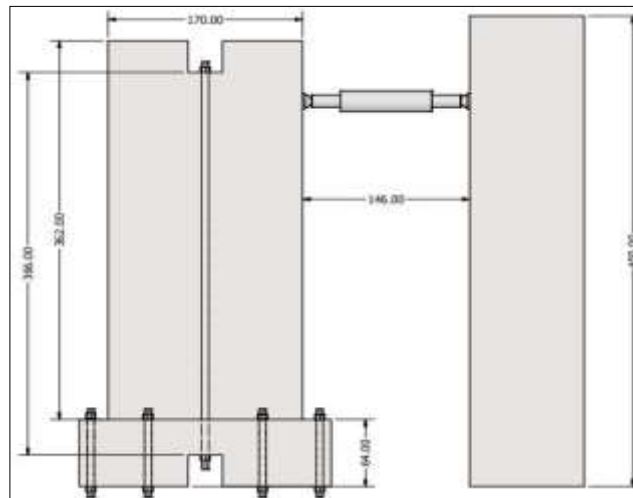


Figure 3. The schematic view of the test sample, the HPWM6, and its dimensions [2]

Table 1. Tensile properties of steel materials

Characteristics	15.24 mm diameter post-tensioned strand	16 mm diameter bar	10 mm diameter bar	8 mm diameter stirrup
Area, mm ²	140	201.1	78.5	50.3
Yield strength, MPa	1650	438	430	451
Strain at yield strength, %	0.85	0.31	0.36	0.43
Peak strength, MPa	2050	620	557	618
Strain at peak strength	5.6	15	12	7.7
Elongation, %	5.6	19	14.3	10.8

Table 2. Tensile, compressive, and shear strength of FRP sheets in different directions [29]

Longitudinal Tensile Strength (Pa)	Longitudinal Compress Strength (Pa)	Transverse Tensile Strength (Pa)	Transverse Compress Strength (Pa)	Longitudinal Shear Strength (Pa)	Transverse Shear Strength (Pa)
2.28×10 ⁹	1.44×10 ⁹	57×10 ⁶	228×10 ⁶	71×10 ⁶	71×10 ⁶

Table 3. Computer models of the walls strengthened with FRP (The main direction of FRP is longitudinal, and FRP thickness is 1.4 mm)

Model	The angle of installation of FRP sheet on the wall	FRP width	FRP length
dfrp02085x1.4	0	20cm	85cm
dfrp452085x1.4	45	20cm	85cm
dfrp902085x1.4	90	20cm	85cm
dfrp04085x1.4	0	40cm	85cm
dfrp454085x1.4	45	40cm	85cm
dfrp904085x1.4	90	40cm	85cm
dfrp020170x1.4	0	20cm	170cm
dfrp4520170x1.4	45	20cm	170cm
dfrp9020170x1.4	90	20cm	170cm
dfrp040170x1.4	0	40cm	170cm
dfrp4540170x1.4	45	40cm	170cm
dfrp9040170x1.4	90	40cm	170cm

A numerical parametric study using the FE modeling method is run to assess the in-plane behavior of the post-tensioned precast RC shear walls strengthened by FRP sheets subject to simultaneous gravity and increasing lateral displacement.

In this research, a finite element model (FEM) was created using ABAQUS to adapt the general behavior of HPWEM samples. In the following, the eight-node C3D8R rigid element with reduced integral is used to model the behavior of concrete, and the element T3D2 linear truss, with two nodes, has been used to model reinforcements and retracted tendons. The plastic behavior of concrete and the ideal multilinear elastoplastic behavior of steel were combined in the built models. The mechanical model of the connection between the wall, the beam, and the foundation is assumed to be a rigid connection in the vertical direction with limited friction and sliding in the tangential direction. It should be noted that this type of modeling simulates the opening/closing behavior of the horizontal connection.

The “Embedded region” constraint is applied to define the concrete and rebar interaction. For the concrete and FRP sheets interaction based on their failure mode, the “Tie” constraint is applied. The interaction between the wall and the foundation is modeled through the “Surface-To-Surface” constraint, with “Rough” tangent behavior and “Hard contact” vertical behavior. This model allows the wall to move vertically on the foundation when subject to compressive stress, thus preventing horizontal sliding. The unbounded tendons are rigidly connected to the top of the wall through the beam type “Multipoint” constraint. The steel anchors are connected to the concrete wall with a “Tie” constraint.

2.2. Validation with Experimental Tests

The results of the nonlinear finite element analysis of the test specimen (HPWEM6) are presented in terms of load and lateral displacement curves and damage distribution in the wall. In Figure 4, the numerical load-displacement curves of the test sample are compared with the backbone curve related to the cyclic test. Based on these curves, the components’ models have acceptable accuracy. Insignificant differences between the load and displacement

curves were obtained for FE analysis and experimental results. It is reasonable due to the test conditions, such as the uncertainty of the loading equipment and measuring instruments, the complex behavior of reinforced concrete as a composite material, and the FE method's inherent characteristics. Similar to the observations in the experiments, the tensile damage distribution in the walls is associated with the energy-dissipating reinforcement's failure, the creation of shear and bending cracks in the wall plate, and the crushing of post-tensioned precast RC shear Walls (Figure 5). The HPWEM provides better strength, stiffness, energy dissipation, and ductility than the monolithic wall specimen. An increase in the strands amount/count (i.e., enlargement of the area of the tendon) enhances the specimen strength and otherwise weakened energy-absorbing capacity and ductility. Shortening the deboned length of grouted reinforcements enhances the specimen's strength, initial stiffness, and ductility. Increasing the tendon's post-tensioned force enhances the initial specimen stiffness and axial load-bearing capacity. It also reduces the specimen's ductility and energy dissipation capacity. The overlapping welded ties with smaller length-to-width ratios improved the concrete confinement property, thus reducing the concrete damage at wall toes. The grouted reinforcements yield is delayed in the wrapped length [2].

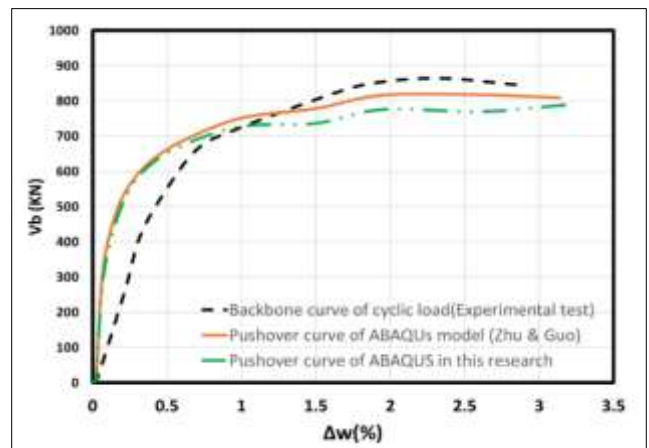


Figure 4. Comparison of numerical and experimental load and displacement curves of HPWEM6

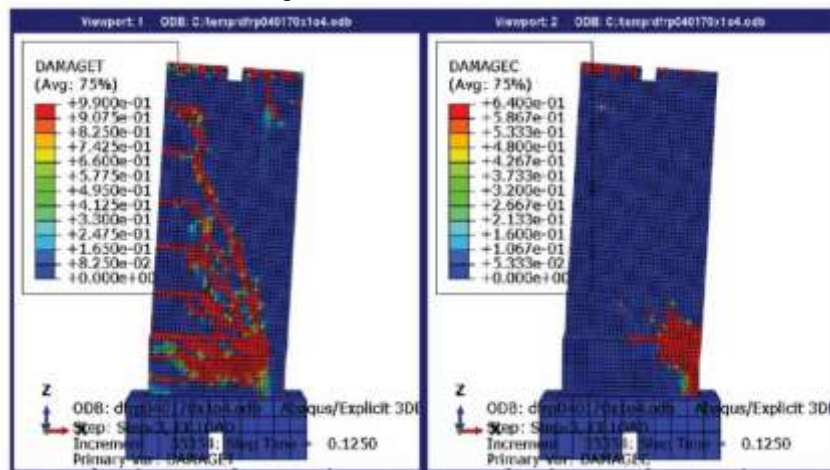


Figure 5. Damage distribution in HPWEM6 wall

2.3. Description of the Sensitivity Analysis

To determine the dimensions of the elements in order to perform sensitivity analysis, computer model analysis has been done in three stages. In each step, the dimensions of the elements were changed, and the results obtained were compared and verified with the experimental results. In these stages, the elements' dimensions were chosen to be 10 cm, 5 cm, and 2.5 cm, respectively. The criterion for choosing the dimensions of the elements for continuing modeling and analysis is that, in addition to having enough accuracy to match the experimental results, choosing the correct size will increase the speed of analysis and reduce the analysis time.

3. Results and Discussion

The data obtained from the modeling of the HPWEM6 wall strengthened with FRP sheets are analyzed to determine the effect of using these sheets on the lateral-load bearing performance of the wall and to realize how the force changes and the relative displacement changes thereof at different stages of the wall's response, and finally to the comparison of the strengthened walls' increased capacity with the non-strengthened (Table 4). Assuming that the FRP sheets act only in tension, for the simplicity of the modeling process, only part of the FRP sheets that are affected by tensile stress is modeled. To shed more light on the findings here, the four situations are considered for connecting the FRP sheets to the wall.

Table 4. Relative displacement force at different response states of walls strengthened with FRP

Model	Parameter	State			
		Decompression state	Softening state	Yielding state	Failure state
dwall	Force (N)	227175	671398	694883	825175
	Capacity Increase %		0		
dfrp902085x1.4	Force (N)	231320	695788	693984	841619
	Capacity Increase %		3.84		
dfrp904085x1.4	Force (N)	233821	689733	662402	793594
	Capacity Increase %		2.01		
dfrp9020170x1.4	Force (N)	237413	707824	708361	860615
	Capacity Increase %		7.07		
dfrp9040170x1.4	Force (N)	230521	711900	742990	924692
	Capacity Increase %		9.91		
dfrp02085x1.4	Force (N)	223822	674818	685213	824544
	Capacity Increase %		1.47		
dfrp04085x1.4	Force (N)	225329	684721	681239	824992
	Capacity Increase %		1.09		
dfrp020170x1.4	Force (N)	230273	699453	704116	847856
	Capacity Increase %		2.64		
dfrp040170x1.4	Force (N)	221795	699452	702818	847391
	Capacity Increase %		4.07		
dfrp452085x1.4	Force (N)	216819	703329	690301	838463
	Capacity Increase %		2.42		
dfrp454085x1.4	Force (N)	211628	705401	687772	831189
	Capacity Increase %		2.86		
dfrp4520170x1.4	Force (N)	218920	709862	707697	845090
	Capacity Increase %		5.56		
dfrp4540170x1.4	Force (N)	225232	720969	713909	859533
	Capacity Increase %		7.23		
dfrp4540170x1.4+ dfrp9040170x1.4	Force (N)	219897	716300	700649	851954
	Capacity Increase %		7.06		
All Models	$\Delta\omega\%$	0.11847	1.48207	2.28491	2.85496

As shown in Figure 2-a, the FRP sheets are installed around and along the border elements of the post-tensioned precast reinforced concrete shear wall perpendicular to the heel of the wall. For the post-tensioned precast reinforced concrete shear walls dfrp9020170x1.4, dfrp904085x1.4,

dfrp9040170x1.4, and dfrp902085x1.4, the analysis results of these walls with horizontal incremental displacement in the form of a relative force-displacement diagram are shown in Figure 6, and the response stages of the wall are tabulated in Table 6.

For example, for the dfrp902085x1.4 concrete wall, it is evident that the response of the dfrp902085x1.4 wall in the decompression State is not much different from the “HPWEM6” wall. In the Softening State, with a relative displacement of 1.8671%, the force volume increases to 696 KN. While in the yielding state, there were few changes, and in the failure state, the force increased to the value of 842 KN with a relative displacement of 2.8550%. Meanwhile, comparing the capacity of the dfrp902085x1.4 wall and HPWEM6, it is clear that the use of FRP sheets increased the capacity of the dfrp902085x1.4 wall by 3.84% compared to HPWEM6.

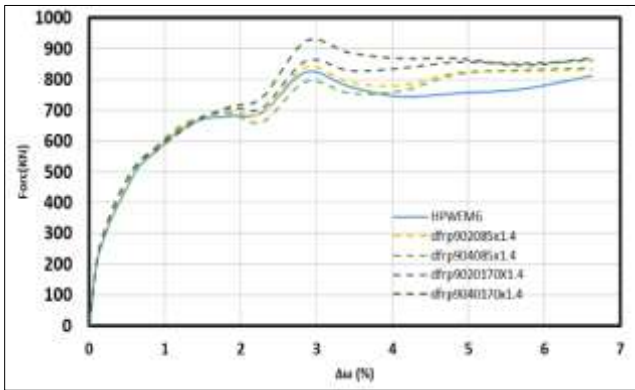


Figure 6. Relative force-displacement diagram of HPWEM6 wall and samples strengthened with FRP sheets parallel to the boundary elements

The FRP sheets and their arrangement are shown in Figure (2-b), whereas observed, they are attached to the concrete wall and parallel to the bottom edge of the wall and the foundation beam. After the failure state, the point defined by the wall failure, due to concrete crushing subject to bending, stiffness increases more in the wall strengthened with FRP sheets than the un-strengthened HPWEM6 wall. The results of the analysis and their comparison regarding the dfrp02085x1.4, dfrp04085x1.4, dfrp020170x1.4, and dfrp040170x1.4 walls are shown in Figure 7. The details are tabulated in Table 4.

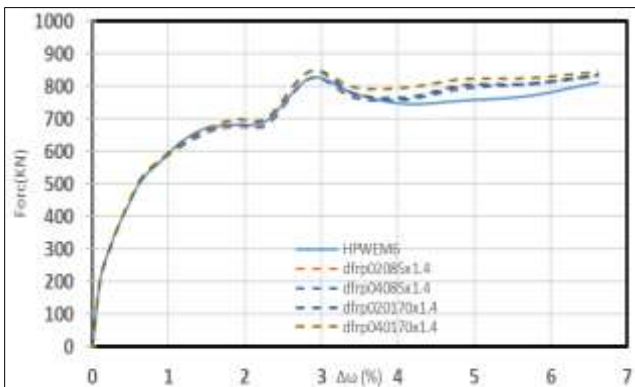


Figure 7. Relative force-displacement diagram of HPWEM6 wall and samples strengthened with FRP sheets perpendicular to boundary elements

In the third primary model of Figure (2-c), the installation angle of the FRP sheets to the lower edge of the wall is 45°, the thickness of the FRP sheets is 1.4 mm, and the width and

length of the sheets are changed as parameters. The performance of wall samples dfrp454085x1.4, dfrp452085x1.4, dfrp4520170x1.4, and dfrp4540170x1.4 only in softening state is different from HPWEM6 concrete wall. In other states, there is no considerable difference in the performance of FRP-strengthened walls with HPWEM6 walls, though strengthening the wall with FRP sheets increases the stiffness and capacity of the walls after the failure state. Part of the tensile stresses caused by the bending and shearing forces in the wall plane are borne by the FRP sheets (Figures 4 and 8).

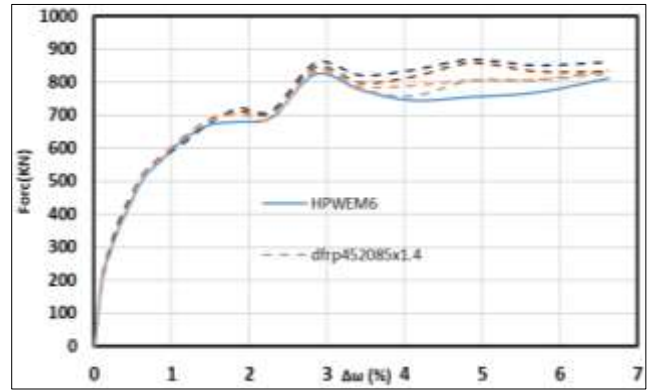


Figure 8. Relative force-displacement diagram of HPWEM6 wall compared to HPWEM6 walls strengthened with FRP sheets at an angle of 45° relative to the top edge of the foundation beam

4. Conclusions

This research is a parametric study based on the data of an experimental study aimed at the effect of FRP sheet arrangement on the performance of post-tensioned precast concrete walls under lateral load. Based on this, finite element models were first created to validate the models, and after ensuring the validation process, secondary models were created with different arrangements of FRP sheets, and sheets with different angles and lengths were examined. Based on this, the research results are as follows:

- The results of the finite element model are in very good agreement with the results presented in the experimental study on the ultimate strength and load-displacement curves. Based on this, it can be said that the models presented in this research are reliable for evaluating and simulating post-tensioned precast concrete walls.
- Comparing the results related to the dfrp02085x1.4, dfrp020170x1.4, dfrp904085x1.4, and dfrp9040170x1.4 walls, where only the length of the sheets is changed, it is revealed that by increasing length, the shear and bending capacity of post-tensioned precast concrete walls will increase. Compared to HPWEM6 for the above-strengthened walls, this increase in capacity is 1.47, 2.64, 2.01, and 9.91%, respectively.
- By comparing the results related to dfrp02085x1.4, dfrp04085x1.4, dfrp9020170x1.4, and dfrp9040170x1.4, walls where only the width of the sheets is changed, it is revealed that an increase in the width of the sheet increases the shear and bending capacity of the concrete

walls. Compared to HPWEM6 for the above-mentioned strengthened walls, the capacity increase values are 1.47, 1.09, 7.07, and 9.91%, respectively.

- The greater the FRP sheets in installation angle on the horizon, the greater the capacity and plasticity of the wall. (i.e., dfrp040170x1.4, dfrp4540170x1.4, and dfrp9040170x1.4). Compared to the HPWEM6, the capacity increase values are 4.07, 7.23, and 9.91%, respectively.
- Applying FRP sheets with the proposed details increased the shear-bending capacity and ductility, improving the post-tensioned precast concrete walls' resistance against lateral-load bearing performance.
- The greatest increase in capacity is related to the FRP sheets at the points where the tensile stresses caused by the shear and bending forces are focused, and the FRP sheets are connected from their main direction and aligned with these stresses.
- By increasing the length and width of the FRP layers, the ductility increases by a maximum of 9.8%. This rate can be observed at all angles, regardless of the angle of the FRP sheet.

5. References

- [1] Palermo, D., & Vecchio, F. J. (2002). Behavior of three-dimensional reinforced concrete shear walls. *ACI Structural Journal*, 99(1), 81–89. doi:10.14359/11038.
- [2] Zhu, Z., & Guo, Z. (2016). Experiments on hybrid precast concrete shear walls emulating monolithic construction with different amounts of posttensioned strands and different debond lengths of grouted reinforcements. *Advances in Materials Science and Engineering*, 2016(6802503). doi:10.1155/2016/6802503.
- [3] Erkmen, B., & Schultz, A. E. (2009). Self-Centering Behavior of Unbonded, Post-Tensioned Precast Concrete Shear Walls. *Journal of Earthquake Engineering*, 13(7), 1047–1064. doi:10.1080/13632460902859136.
- [4] Singhal, S., Chourasia, A., Chellappa, S., & Parashar, J. (2019). Precast reinforced concrete shear walls: State of the art review. *Structural Concrete*, 20(3), 886–898. doi:10.1002/suco.201800129.
- [5] Greifenhagen, C., & Lestuzzi, P. (2005). Static cyclic tests on lightly reinforced concrete shear walls. *Engineering Structures*, 27(11), 1703–1712. doi:10.1016/j.engstruct.2005.06.008.
- [6] Boulekbache, B., Hamrat, M., Chemrouk, M., & Amziane, S. (2012). Influence of yield stress and compressive strength on direct shear behaviour of steel fibre-reinforced concrete. *Construction and Building Materials*, 27(1), 6–14. doi:10.1016/j.conbuildmat.2011.07.015.
- [7] Sakr, M. A., El-Khoriby, S. R., Khalifa, T. M., & Nagib, M. T. (2017). Modeling of RC shear walls strengthened by FRP composites. *Structural Engineering and Mechanics*, 61(3), 407–417. doi:10.12989/sem.2017.61.3.407.
- [8] El-Sokkary, H., Galal, K., Ghorbanirenani, I., Léger, P., & Tremblay, R. (2013). Shake Table Tests on FRP-Rehabilitated RC Shear Walls. *Journal of Composites for Construction*, 17(1), 79–90. doi:10.1061/(asce)cc.1943-5614.0000312.
- [9] Cortés-Puentes, W. L., & Palermo, D. (2012). Modeling of RC Shear Walls Retrofitted with Steel Plates or FRP Sheets. *Journal of Structural Engineering*, 138(5), 602–612. doi:10.1061/(asce)st.1943-541x.0000466.
- [10] Deng, K., Pan, P., Shen, S., Wang, H., & Feng, P. (2018). Experimental Study of FRP-Reinforced Slotted RC Shear Walls under Cyclic Loading. *Journal of Composites for Construction*, 22(4). doi:10.1061/(asce)cc.1943-5614.0000855.
- [11] Shen, D., Yang, Q., Jiao, Y., Cui, Z., & Zhang, J. (2017). Experimental investigations on reinforced concrete shear walls strengthened with basalt fiber-reinforced polymers under cyclic load. *Construction and Building Materials*, 136, 217–229. doi:10.1016/j.conbuildmat.2016.12.102.
- [12] Triantafyllou, T. C. (1998). Strengthening of Masonry Structures Using Epoxy-Bonded FRP Laminates. *Journal of Composites for Construction*, 2(2), 96–104. doi:10.1061/(asce)1090-0268(1998)2:2(96).
- [13] Sonobe, Y., Fukuyama, H., Okamoto, T., Kani, N., Kimura, K., Kobayashi, K., Masuda, Y., Matsuzaki, Y., Mochizuki, S., Nagasaka, T., Shimizu, A., Tanano, H., Tanigaki, M., & Teshigawara, M. (1997). Design Guidelines of FRP Reinforced Concrete Building Structures. *Journal of Composites for Construction*, 1(3), 90–115. doi:10.1061/(asce)1090-0268(1997)1:3(90).
- [14] Lombard, J. C. (1999). Seismic strengthening and repair of reinforced concrete shear walls using externally bonded carbon fibre tow sheets. PhD Thesis, Carleton University, Ottawa, Canada.
- [15] Khalifa, A., Gold, W. J., Nanni, A., & M.I., A. A. (1998). Contribution of Externally Bonded FRP to Shear Capacity of RC Flexural Members. *Journal of Composites for Construction*, 2(4), 195–202. doi:10.1061/(asce)1090-0268(1998)2:4(195).
- [16] Mander, J. B., & Cheng, C. T. (1997). Seismic resistance of bridge piers based on damage avoidance design. Seismic resistance of bridge piers based on damage avoidance design. Technical Report NCEER (97-0014), National Center for Earthquake Engineering Research (NCEER), University at Buffalo, New York, United States.
- [17] Priestley, M. J. N., Sritharan, S. (Sri), Conley, J. R., & Stefano Pampanin, S. (1999). Preliminary Results and Conclusions From the PRESSS Five-Story Precast Concrete Test Building. *PCI Journal*, 44(6), 42–67. doi:10.15554/pci.11011999.42.67.
- [18] Tanyeri, A. C. (2014). Seismic performance and modeling of reinforced concrete and post-tensioned precast concrete shear walls. PhD Thesis, University of California, Berkeley, United States.

- [19] Smith, B. J., Kurama, Y. C., & McGinnis, M. J. (2011). Design and Measured Behavior of a Hybrid Precast Concrete Wall Specimen for Seismic Regions. *Journal of Structural Engineering*, 137(10), 1052–1062. doi:10.1061/(asce)st.1943-541x.0000327. Structural Division, 98(12), 2805–2810. doi:10.1061/jsdeag.0003404.
- [20] Kurama, Y., Sause, R., Pessiki, S., & Lu, L. W. (1999). Lateral load behavior and seismic design of unbonded post-tensioned precast concrete walls. *ACI Structural Journal*, 96(4), 622–632. doi:10.14359/700.
- [21] Holden, T., Restrepo, J., & Mander, J. B. (2003). Seismic Performance of Precast Reinforced and Prestressed Concrete Walls. *Journal of Structural Engineering*, 129(3), 286–296. doi:10.1061/(asce)0733-9445(2003)129:3(286).
- [22] Restrepo, J. I., & Rahman, A. (2007). Seismic Performance of Self-Centering Structural Walls Incorporating Energy Dissipators. *Journal of Structural Engineering*, 133(11), 1560–1570. doi:10.1061/(asce)0733-9445(2007)133:11(1560).
- [23] Perez, F. J., Sause, R., & Pessiki, S. (2007). Analytical and Experimental Lateral Load Behavior of Unbonded Posttensioned Precast Concrete Walls. *Journal of Structural Engineering*, 133(11), 1531–1540. doi:10.1061/(asce)0733-9445(2007)133:11(1531).
- [24] Perez, F. J., Pessiki, S., & Sause, R. (2013). Experimental lateral load response of unbonded post-tensioned precast concrete walls. *ACI Structural Journal*, 110(6), 1045–1055. doi:10.14359/51686159.
- [25] Kuzik, M. D., Elwi, A. E., & Cheng, J. J. R. (2003). Cyclic Flexure Tests of Masonry Walls Reinforced with Glass Fiber Reinforced Polymer Sheets. *Journal of Composites for Construction*, 7(1), 20–30. doi:10.1061/(asce)1090-0268(2003)7:1(20).
- [26] Smith, S. T., Hu, S., Kim, S. J., & Seracino, R. (2011). FRP-strengthened RC slabs anchored with FRP anchors. *Engineering Structures*, 33(4), 1075–1087. doi:10.1016/j.engstruct.2010.11.018.
- [27] Saloo, M., & Kabir, M. Z. (2016, October). Evaluation of Shear-Deficient RC Beams Strengthened by Externally Bonded FRP Sheets Subjected to Impact Loading. *Proceedings of the 5th National and 1st International Conference on Modern Materials and Structures in Civil Engineering*, 26-27 October, 2016, Tehran, Iran.
- [28] Meghdadian, M., Masoodi, A. R., & Ghalehnovi, M. (2024). Experimental study to unraveling the seismic behavior of CFRP retrofitting composite coupled shear walls for enhanced resilience. *Composites Part C: Open Access*, 15(100523). doi:10.1016/j.jcomc.2024.100523.
- [29] Heydari, P., Mostofinejad, D., Eftekhar, M. R., & Saljoughian, A. (2024). Seismic flexural rehabilitation of RC coupling beams with FRP sheets: Evaluation of EBROG technique. *Structures*, 68, 107076. doi:10.1016/j.istruc.2024.107076.
- [30] Kent, D. C., & Park, R. (1972). Closure to “Flexural Members with Confined Concrete.” *Journal of the*